

Figure S1. Histopathological and IHC findings of the primary breast tumor and CT-guided pelvic biopsy. (A-F) Photomicrographs of the primary breast tumor (invasive ductal carcinoma): (A) H&E staining (x100 magnification); (B) Estrogen receptor-positive (IHC; x100 magnification); (C) progesterone receptor-positive (IHC; x100 magnification); (D) HER2-negative (IHC; x100 magnification); (E) Ki-67 proliferative index ~20% (IHC; x100 magnification); (F) Photomicrograph (H&E; x100 magnification) of the CT-guided pelvic biopsy performed in July 2021, showing fragments of cortical bone, inflammatory exudate and necrotic bone, with no malignant cells identified. IHC, immunohistochemistry.

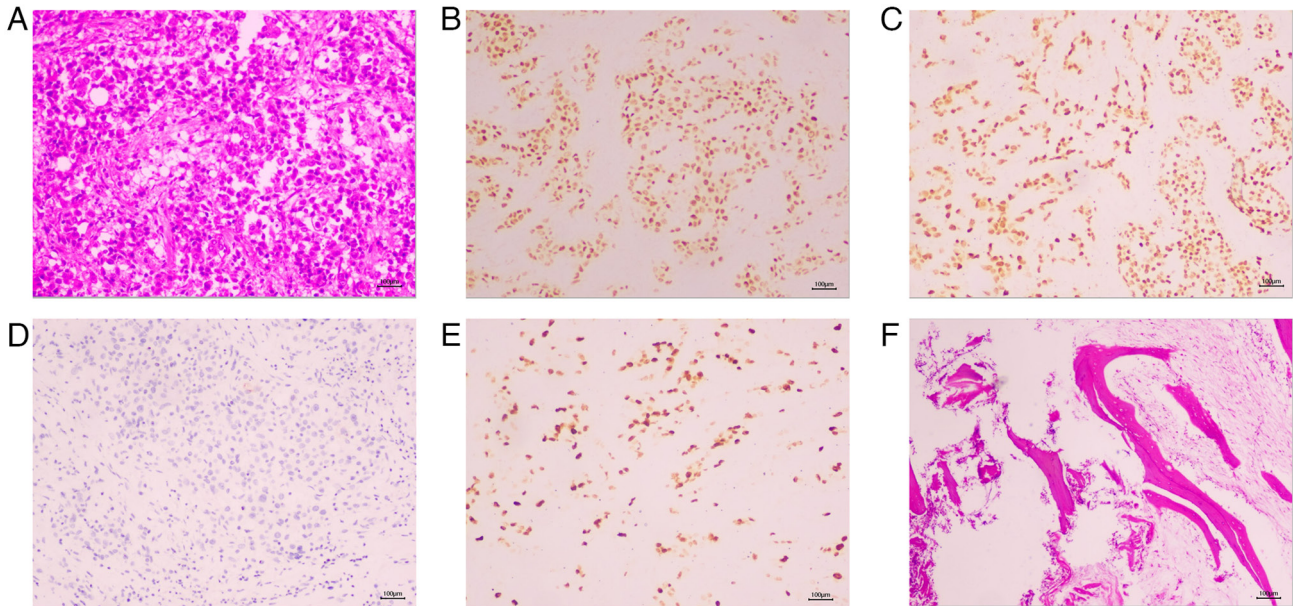


Figure S2. Chest CT and bone scintigraphy findings suggestive of osseous metastases. (A and B) Representative images from a chest CT scan (bone window) performed in December 2019, showing multiple punctate and patchy sclerotic densities involving the bilateral humeral heads, scapulae, sternum, thoracic vertebral bodies and portions of the ribs, suggestive of osseous metastases. (C) Whole-body bone scan revealing multiple foci of increased metabolic activity throughout the skeleton, highly indicative of metastatic disease.

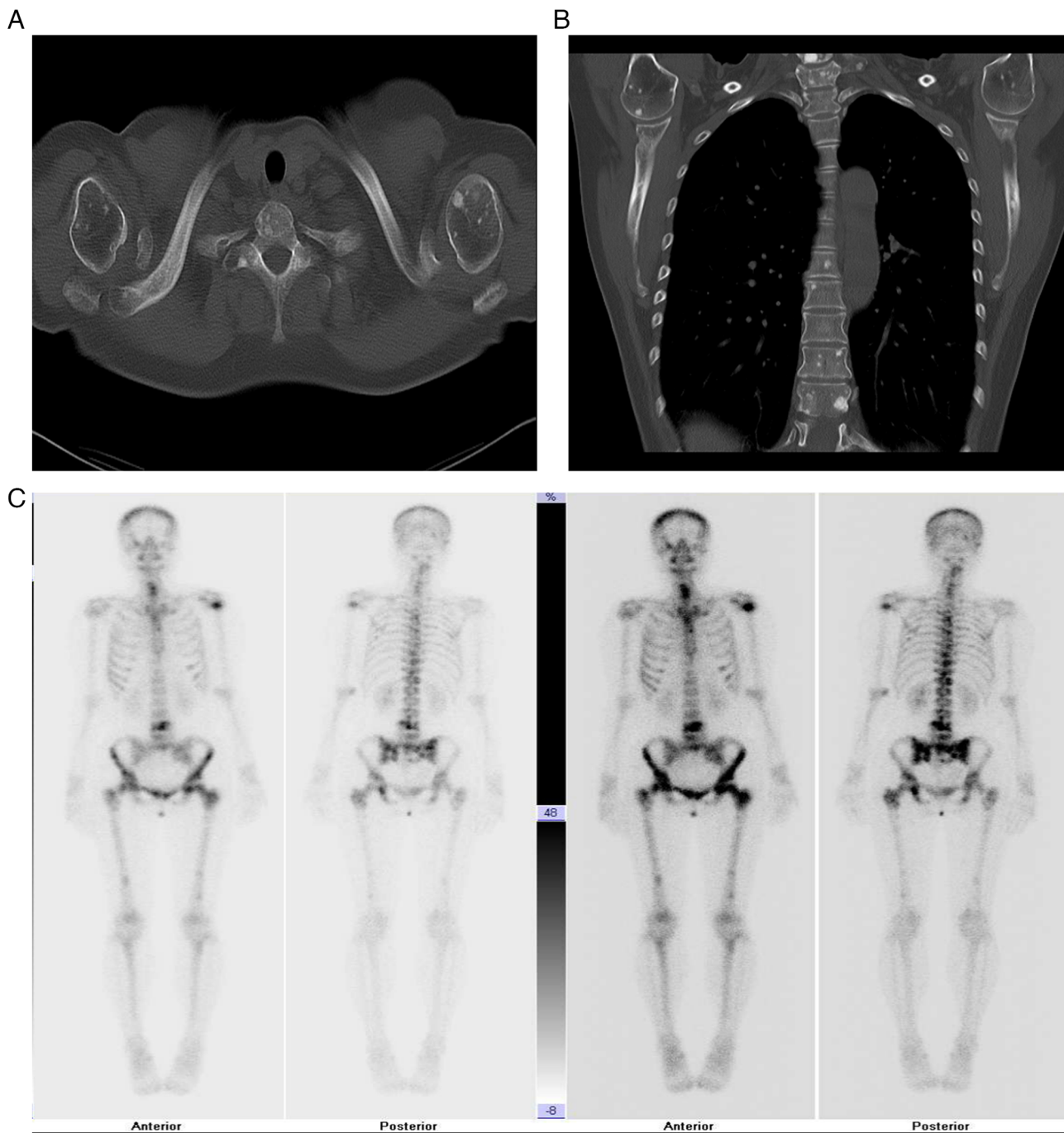


Figure S3. Spinal MRI demonstrating progression of bony metastases. (A and B) Spinal MRI performed in December 2019: (A) T1WI showing scattered speckled and patchy abnormal signals in multiple vertebrae; (B) T2WI with corresponding signal abnormalities. (C and D) Follow-up spinal MRI performed in October 2021: (C) T1WI and (D) T2WI demonstrating unequivocal progression of bony lesions. WI, weighted image.

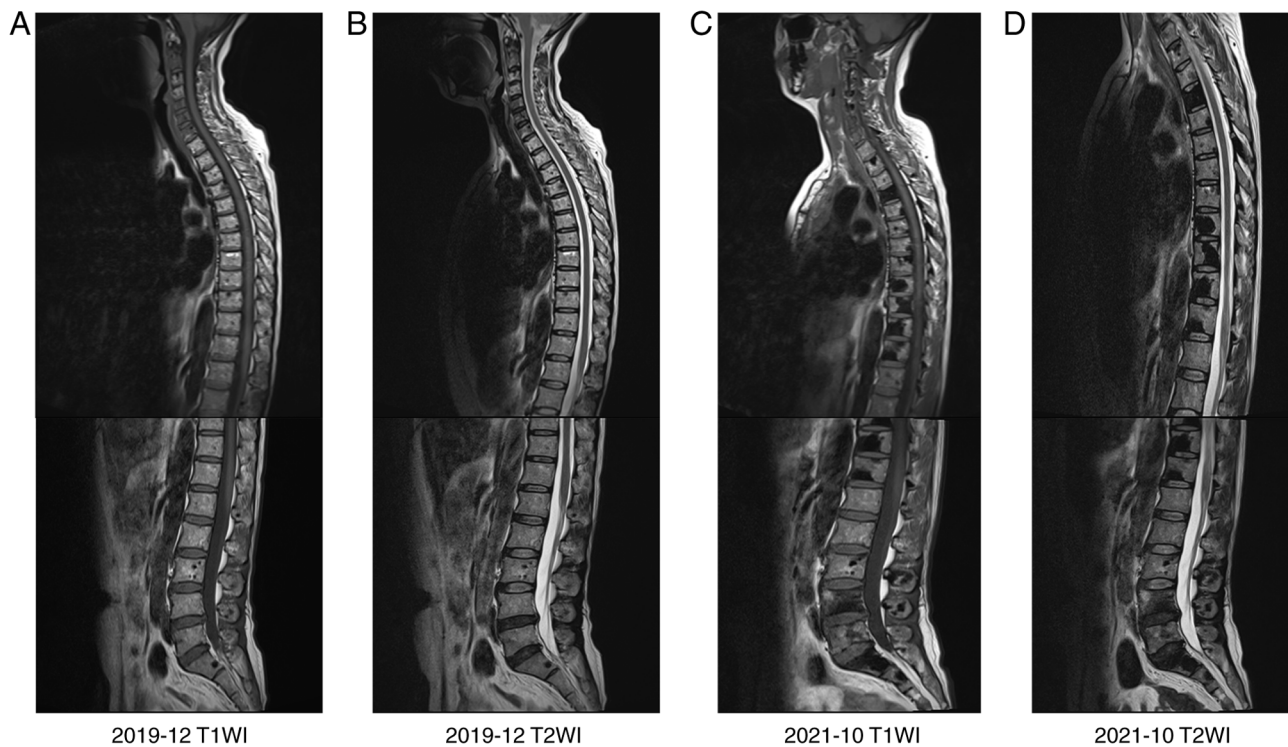


Figure S4. Longitudinal trends of serum tumor markers. Graph showing the dynamic changes in serum levels of CEA, CA125 and CA15-3 from the diagnosis of bone metastasis (December 2019) to the diagnosis of peritoneal disease (January 2022). CEA, carcinoembryonic antigen; CA, carbohydrate antigen.

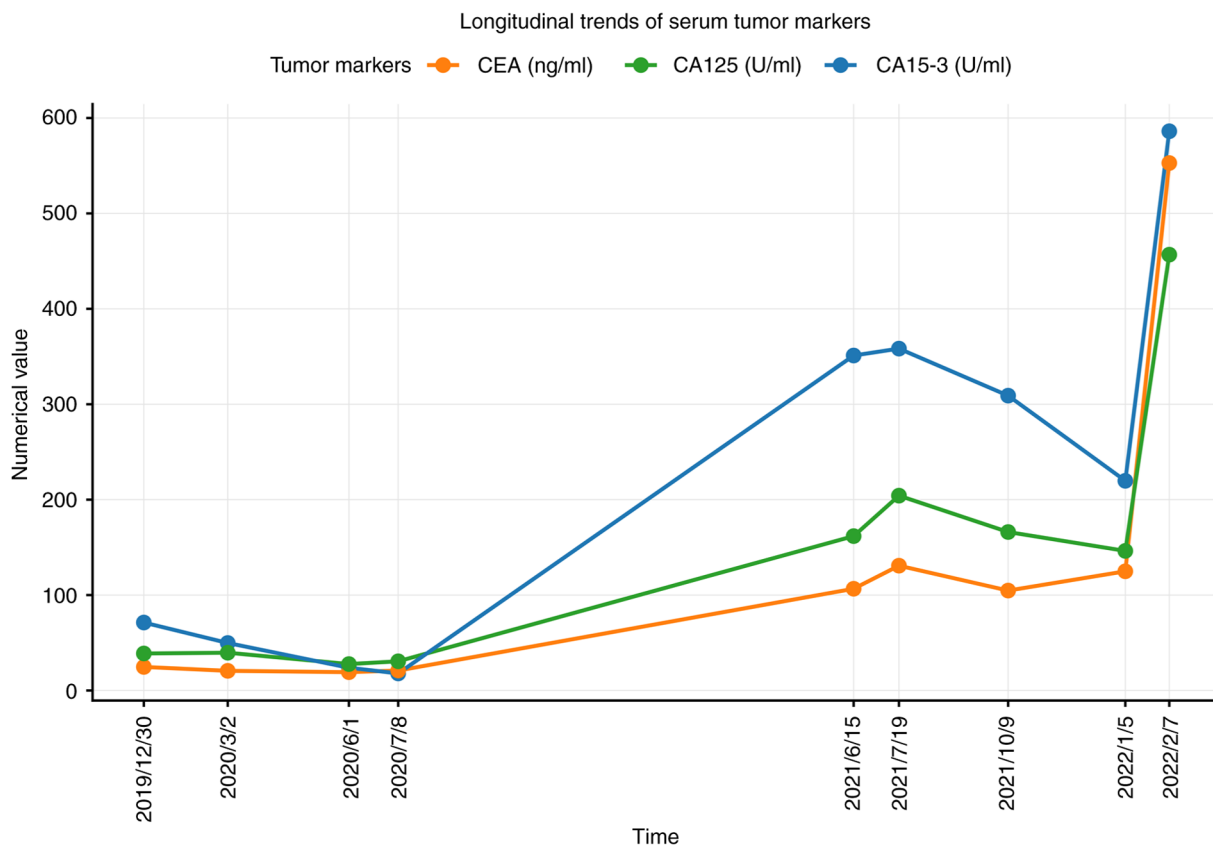


Figure S5. Contrast-enhanced abdominal CT imaging demonstrating peritoneal involvement. (A) Axial CT image shows thickening and stranding of the mesentery (arrow). (B) Axial CT image reveals nodular changes and thickening of the omentum. (C) Coronal CT image depicts newly identified implant-like nodules on the peritoneal surface (arrow). These findings are consistent with peritoneal carcinomatosis.

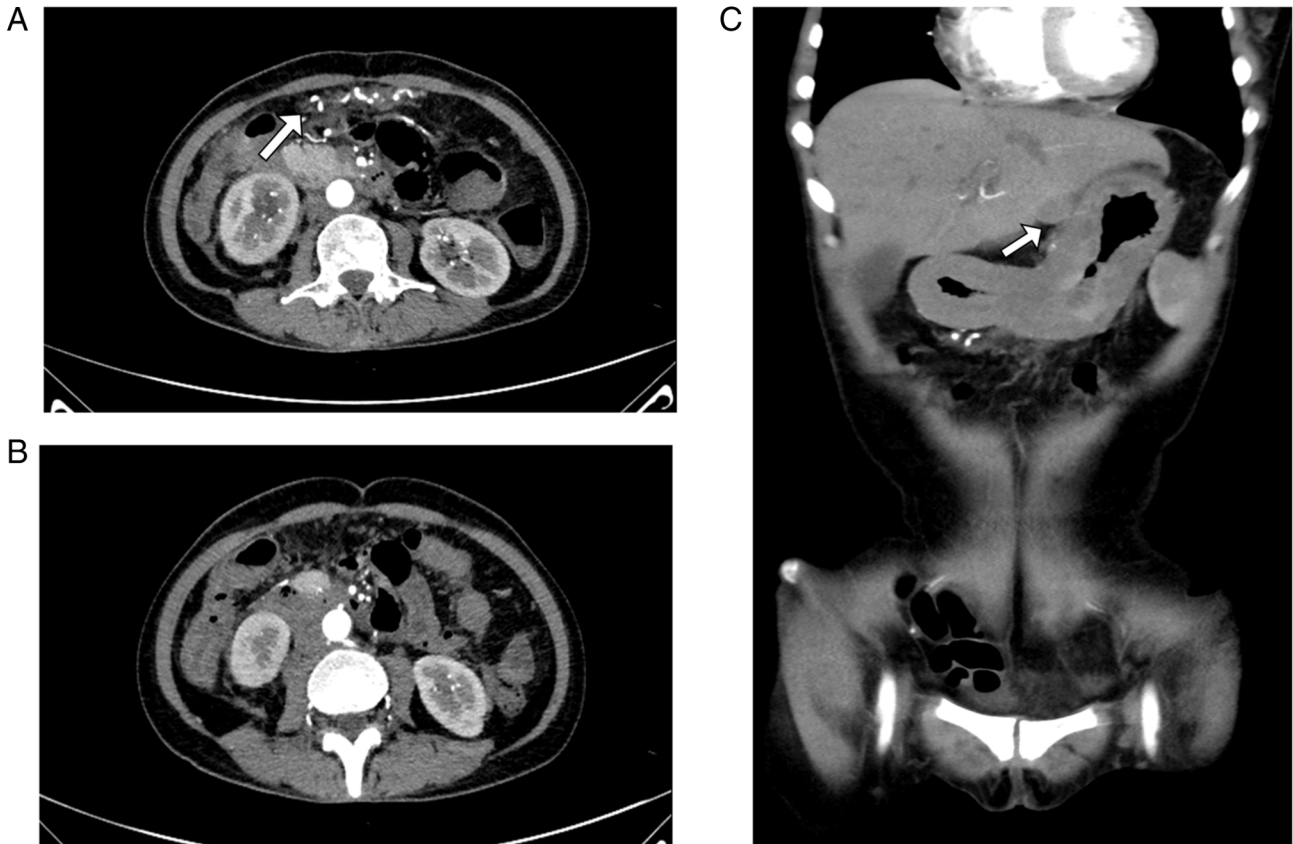


Figure S6. IHC staining for Ki-67. Photomicrograph (IHC; magnification, x100) shows a Ki-67 proliferative index of ~40% in the tumor cells from the omental biopsy. IHC, immunohistochemistry.

